Graphene layered systems as a terahertz source with tuned frequency

K. Batrakov and S. Maksimenko

Phys. Rev. B **95**, 205408 — Published 8 May 2017

DOI: 10.1103/PhysRevB.95.205408

Graphene layered systems as the terahertz source with tuned frequency

K. Batrakov* and S. Maksimenko
Institute for Nuclear Problems, Belorussian State University, Bobruiskaya 11, 220050 Minsk, Belarus

Propagation of an electron beam over a graphene/dielectric sandwich structure is considered assuming the distance between layers to be large enough to prevent interlayer tunnelling. A dispersion equation for the surface electromagnetic modes propagating along graphene sheets is derived and Čerenkov synchronism between surface wave and non-relativistic electron beam is predicted at achievable parameters of the system. The generation frequency tuning is proposed by varying the graphene doping, the number of graphene sheets, the distance between sheets, etc.

PACS numbers: 41.60.-m,78.67.Ch,73.63.Fg

I. INTRODUCTION

Due to a variety of scientific and technical applications, there is a great need in the development of coherent terahertz radiation sources with tunable frequency, see e.g. Refs. 1,2 and references therein. In particular, the tunability can be realized in the devices utilizing kinetic energy of moving electrons and transforming it into the energy of the emitted electromagnetic wave[3]. Free electron laser (FEL)[4], travelling wave tube (TWT) and backward wave oscillator (BWO), are the well-known devices of such a type. The energy transfer occurs when parameters of the electron beam moving with the velocity $\mathbf{u}$ and the electromagnetic wave meet the synchronism condition (for example $\omega - \mathbf{ku} = 0$ in Čerenkov case). Changing electron velocity one can smoothly tune the frequency in a wide range. The development of FELs was initiated, in particular, by this feature. However, the electron beam sources are normally optimized for working at a given electron energy and do not allow its easy variation without considerable efficiency drop. Instead, the tunability could be achieved by exposing the medium which provides the synchronization conditions to external fields – for example, by varying the undulator magnetic field[4] – but again this way appears to be rarely used in practice since undulator is usually designed for a given operating frequency and its efficiency significantly drops with deviation.

In the case of Čerenkov-type emitter[5], the radiation frequency depends *also* on electrodynamic parameters of the medium providing thus alternative means of the resonant frequency tuning. Among different possibilities, graphene and carbon nanotubes (CNTs) are very promising materials from this point of view since there are well-known and rather facile methods of their constitutive parameters wide-range varying. In particular, well-developed methods of graphene doping inclusive of electrostatic doping allow smooth alteration of the surface conductivity[6]. Analogous effect is reported in doped CNTs[7,8]. Besides, it has been shown that carbon nanotubes and graphene can considerably slow down surface electromagnetic wave[9,10] providing thus better conditions for the synchronization of electron beam and electromagnetic surface wave.

Čerenkov mechanism of generation of the coherent stimulated radiation in graphene and carbon nanotubes was theoretically investigated in Refs. 10–15 demonstrating realizability of the nanotube-based nano-TWT and nano-FEL at realistic parameters of CNTs and electron beams[14]. In literature has also been discussed the mechanism of generation and amplification of plasmon oscillations in graphene by optical or electrical pumping[16–21]. Efficiency of emission and influence of quantum recoil effect on Čerenkov emission by hot electrons in graphene were studied in Refs. 22,23. A possibility of terahertz emission in CNTs imposed to transverse and axial electric fields due to electric-field induced heating of electron gas has been revealed in Refs. 24–28. A periodical systems of graphene nanoribbons has been proposed as Čerenkov medium with regulation of generation frequency by nanoribbon width, spatial period and applied voltage[29,30]. A similar approach exploiting periodic dielectric substrate underlaying graphene sheet has been developed in Refs. 31,32. Variant with analogous to Čerenkov radiation due to excitation of dipole polarization an the array of nanotubes which leads to current generation with a superluminal profile is considered in Refs. 33,34.

Unique physical properties of graphene, plane or rolled up into cylinder, are featured in that not only external electron beam can be used for excitation of surface waves but also graphene's own π electrons[10,14,29]. There are several reasons in favor of such a generation scheme: First, graphene and nanotubes support extraordinary large continuous electric current density, $> 10^8$ A/cm^2, without degradation, see e.g. Refs. 35–37. Then, macroscopically large ballistic length (up to several hundred microns) in graphene and nanotubes is reported[38–41]. For example, about 16 micron length electron ballistic transport in graphene nanoribbons has recently been observed[42]. Therefore, electrons can emit coherently from this macroscopic length. Physical basis of such a high ballisticity is in Dirac nature of graphene carriers and Klein paradox[43,44] which helps to overcome the potential barriers. Lastly, metallic CNTs exhibit a strong, as large as 50-100 times, slowing down of surface electromagnetic waves[9]. In single layer graphene this quantity appears to be smaller but below we show that this prob-

lem can be resolved using slow acoustic mode in multi-layered structure due to coupling of plasmon-polariton modes of different layers[10]. Similar effect can be achieved by hybridization of graphene plasmon with its mirror image in the metal plate disposed near graphene layer that leads, in particular, to strongly confined asymmetric mode[45,46]. Thus, as it has been stressed in Ref.14, a combination in graphene and CNTs of three key properties, (i) ballisticity of the electron flow over typical length, (ii) extremely high current-carrying capacity, and (iii) strong slowing down of surface electromagnetic waves[9], allows proposing them as candidates for the development of nano-sized Černekov-type emitters. As our estimates show[14],the electron mean free path as large as tens of microns would be enough to provide coherent emission and reach the above stated goal. However, practical realization of such a large ballistical transport is a complicated task and, in any case, is inconsistent with the high current density.

Alternatively, traditional Černekov and Smith-Purcell generation scheme can be utilized, when an external electron beam moves synchronously with the excited surface wave over the graphene surface on the distance sufficient to neglect electron collisions with carbon atoms. Later condition allows exclude negative role of electrons multiple scattering which destroys Čerenkov synchronism. To provide necessary slowing down we propose to make use a sandwich structure consisted of parallel noninteracting graphene layers. In Ref. 10 we have shown that in two spatially separated graphene layers one of the surface plasmonic modes can be significantly slowed down, up to the velocity of graphene π-electrons. Moreover, a new mechanism of the frequency tuning appears exploiting the interlayer distance varying. Recently[47,48] we have demonstrated a strong graphene interaction with radiation. In particular, free standing single graphene layer can absorb up to 50% of exposing radiation intensity in microwave and terahertz frequency ranges. This percentage can be significantly increased under corresponding choice of the substrate. From the Einstein rules follows that the inverse process, i.e. stimulated radiation emission, can proceed equally effectively.

In the present paper we study excitation of surface waves propagating in graphene sandwich structures and resonantly interacting with an electron beam, aiming at the reveal of the generation conditions and methods of the smooth frequency tuning by variation of the system parameters. The remainder of the paper is organized as follows. In Sect. II the problem formulation and basic equations are presented. A solution of the boundary-value problem for a single layer graphene sheet, possibility of electromagnetic wave slowing down and frequency tuning in that case is presented in Sect. III. Section IV presents results concerning surface electromagnetic wave in two-layer graphene system, enhanced wave slowing down for acoustical mode and addictive change of effective chemical potential for optical mode. Both these effects give possibility to regulate the generated frequency and resonance electron beam energy. Dispersion equation for graphene system with external electron beam is presented in V. Solution of this equation gives increment of instability and estimation of required for generation parameters. Sect. VI contains analysis concerning possibilities of generation and frequency tuning based on previous calculations and conclusion remarks.

II. BASIC EQUATIONS

Consider an electron beam propagating along the x axis parallel to a graphene sheet or multi-layer graphene sandwich structure comprising graphene sheets separated by layers of a mediums with dielectric functions ε_i. The index i marks the double layer graphene+underlying medium in the sandwich, see Fig. 1. On its way over the sandwich the beam interacts with the surface electromagnetic wave retained by the graphene structure. For the coherent radiation generation, the beam motion should be synchronized with the electromagnetic wave on the beam propagation length over the structure. In particular, for the Čerenkov emission mechanism the electron beam velocity must coincide with the phase velocity v_{ph} of electromagnetic wave. That is, since the electron velocity is smaller the speed of light, the surface wave slowing down is the necessary condition of synchronization.

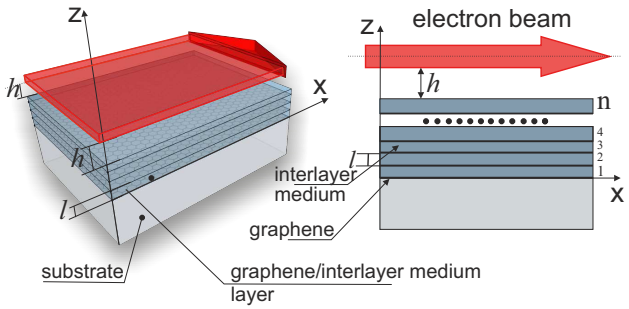

FIG. 1: Geometry of the problem

Let us examine propagation of surface waves along the sandwich in free space, assuming the distances between graphene layers large on the atomic scale and, therefore, neglecting electron interlayer tunnelling in the sandwich. Further we follow the procedure developed in Refs.[47–49]. The eigenwaves under study satisfy the Maxwell equations, boundary conditions at the graphene surfaces in each layer, and the condition that there are no exterior current sources at infinity. From the Maxwell equations we express the field of TM wave in piecewise continuous form:

$$H_y^{(i)} = e^{iqx}\left(c_1^{(i)}\exp\{ik_z^{(i)}z\} + c_2^{(i)}\exp\{-ik_z^{(i)}z\}\right). \quad (1)$$

Here axis z is perpendicular to the graphene layers, $k_z^{(i)} = \sqrt{\omega^2\varepsilon_i/c^2 - q^2}$ is the z-projection of the wave vec-

tor in the i-th layer, $\mathbf{q}$ is the tangential component of the wave vector. Further we assume $\varepsilon_i = 1$. Generalization the case $\varepsilon_i \neq 1$ can easily be performed and, what is important, does not bring to essential changes. To find the surface eigenmodes we need to determine the unknown coefficients $c^{(i)}$. The boundary conditions state continuity of the electric field tangential component on the graphene surface while tangential component of magnetic field undergoes discontinuity proportional to the surface current $\mathbf{j}_t$ excited in graphene[47–49]:

$$\mathbf{H}\left(z_i + 0\right) - \mathbf{H}\left(z_i - 0\right) = \frac{4\pi}{c}\left[\mathbf{j}_t\left(z_i\right) \times \mathbf{n}\right]. \qquad (2)$$

Here $\mathbf{n}$ is the unit vector along the z axis. As it has been shown in Ref.[49], the surface current excited in graphene layer is related to the electric field by

$$\mathbf{j}_t = \sigma \mathbf{E}_t = \alpha g_s g_v \frac{T}{\pi\hbar} \ln\left[2\cosh\left(\frac{\mu}{2T}\right)\right] \frac{ic}{\omega + i\Gamma}\mathbf{E}_t\,, \quad (3)$$

where σ is the sheet conductivity of graphene monolayer, μ is the chemical potential of electron subsystem, T is the temperature in energy units, Γ is the broadening parameter (collision frequency), and α is the fine structure constant. In further calculations we assume $\Gamma \sim 10$ THz in accordance with our previous experiments on the electromagnetic radiation absorption in graphene sandwich structures[47,48]. Note that in our approach any deviations of graphene from idealness (defects, doping, strains, nonhomogeneities, etc.) are taken into account by variation of chemical potential and broadening parameter Γ.

The coefficients g_s and g_v are due to spin and valley degenerations[49] and for graphene can be accepted both as equal 2. In Eq. (3)we only restrict ourselves to intraband transitions. At realistic values of chemical potential this is correct for the terahertz and microwave frequency ranges and inapplicable in optical and NIR ranges where interband transitions come into play. If chemical potential proves to be less the operating frequency, interband transitions should also be accounted for even at low frequencies. However, to reach such a situation special efforts are required during the graphene synthesis and storage[50].

III. SURFACE WAVES IN SINGLE-LAYER SYSTEM

Applying the procedure described to the sandwich structure consisting of n layers, we arrive at the homogeneous system of $2n$ linear equations for $2n$ coefficients $c^{(i)}_{1,2}$. Dispersion equation of the system arises when we set the determinant of the system equal to zero and determines the frequency dependence of the surface wave wavevector. For single graphene layer the system comprises 2 equations for 2 coefficients:

$$c_2 + c_1 = 0\,, \qquad c_2(1 + \sigma_0) - c_1 = 0\,. \qquad (4)$$

Here $\sigma_0 = (4\pi/\omega)k_z\sigma$ is a dimensionless parameter with σ given by Eq. (3) under assumption $g_s, g_v = 2$. Assuming chemical potential considerably exceeding the temperature, from (4) follows the equation

$$\frac{2\mu\alpha}{\hbar\omega}\,\frac{\sqrt{q^2c^2 - \omega^2}}{\omega + i\Gamma} = 1\,, \qquad (5)$$

which describes dispersion of surface electromagnetic wave propagating in graphene. Dispersion equation (5) leads to

$$q^2c^2 = \omega^2 + \left[\frac{\hbar\omega\left(\omega + i\Gamma\right)}{2\mu\alpha}\right]^2. \qquad (6)$$

This equation demonstrates frequency dependence of the surface wave wavevector characteristic for degenerated 2D quantum systems. In the case of potential fields, when we can neglect the first term in the right-hand part of Eq. (6), we arrive at the dependence[51] $q \sim \omega^2$ or $\omega \sim \sqrt{q}$). Note that such a dependence drastically differs from the dependence inherent in the 3D case where eigenfrequency is proportional the Langmuir plasma frequency and does not depend on the wavevector[52]. Specific dispersion law admits strong slowing down of surface waves in 2D systems. The slowing down of surface wave at different μ is

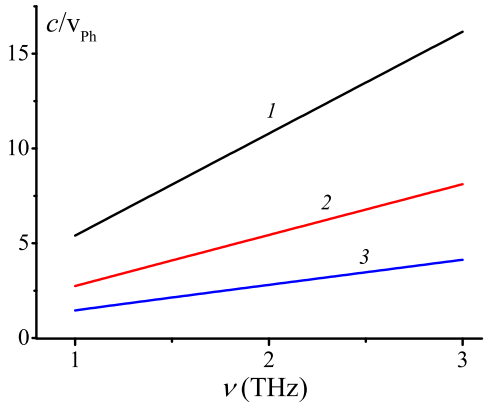

FIG. 2: The phase velocity slowing down for surface wave in an isolated graphene layer for different values of the chemical potential: $\mu = 0.05$ eV (*1*), $\mu = 0.1$ eV (*2*), $\mu = 0.2$ eV (*3*).

illustrated by Fig. 2. It is seen that the effect can vary in a wide range of values depending on the frequency and chemical potential.

The dependence of the Čerenkov resonant frequency (the frequency corresponding to the synchronism condition) ν on chemical potential is depicted on Fig. 3 at different values of the electron beam energy. Fig. 4 demonstrates the Čerenkov resonant frequency variation by changing the electron beam energy. Calculations were made for typical value of the chemical potential $\mu = 0.1$ eV and $\mu = 0.2$ eV.

In the above analysis we considered the TM wave, whose magnetic field vector is coplanar with graphene

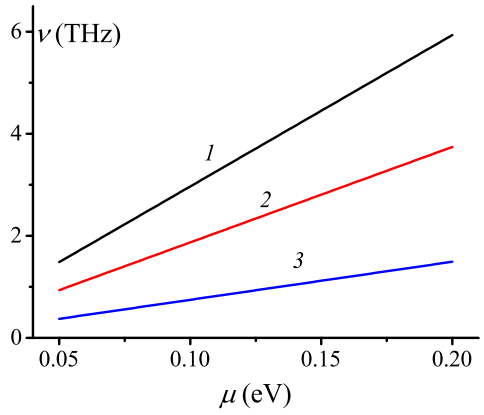

FIG. 3: Čerenkov resonant frequency *vs* chemical potential at the electron beam energy 4 KeV (1), 10 KeV (2) and 60 KeV (3).

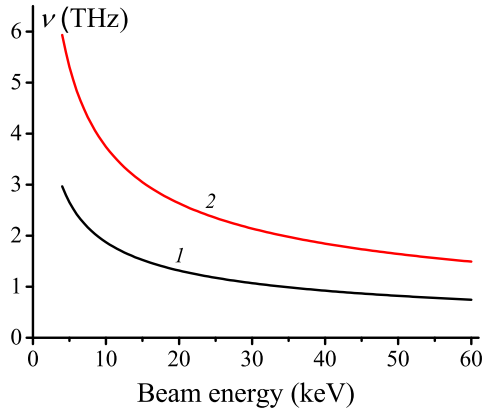

FIG. 4: The Čerenkov frequency dependence on the electron beam energy. Chemical potential $\mu = 0.1$ eV (1) and $\mu = 0.2$ eV (2).

and wavevector is normal to magnetic field. Analogously, boundary conditions can stated for TE wave and corresponding dispersion equation can be obtained:

$$\frac{4\mu\alpha}{\hbar\sqrt{q^2c^2-\omega^2}}\,\frac{\omega}{\omega+i\Gamma}=-2\,. \tag{7}$$

see (5) for comparison. Since TE wave can exist only when the real part of $\sqrt{q^2c^2-\omega^2}$ is positive, from (7) one can conclude that graphene does not supports TE wave in the frequency range under consideration. Excitation of TE waves in isolated graphene layer is possible at much higher frequencies when contribution of interband transitions becomes significant[53].

IV. SURFACE WAVES IN DOUBLE-LAYER SYSTEM

A double-layer graphene system can be used for the generation of Čerenkov radiation by an electron beam[10]. The advantage being achieved by graphene doubling is the appearance of the acoustic mode among plasmon oscillations inherent in the system. This mode whose frequency is proportional to difference of frequencies of plasmonic oscillations in layers. As a result, the phase velocity of this wave appears to be much less than that achievable in monolayer. Owing to such a large slowing down one can meet the Čerenkov synchronism even for graphene π electrons whose velocity is ≈ 300 less then the speed of light.

It should be noted that the Eq. (3) for surface conductivity deduced in Ref. 49 holds only true if $\omega \gg qv_F$. If this condition is not valid, a more precise expression for conductivity should be applied, see Eq. (39) in Ref. 10:

$$\begin{aligned}\sigma' &= \alpha g_s g_v \frac{T}{\pi\hbar}\log\left[2\cosh\left(\frac{\mu}{2T}\right)\right]\frac{ic(\omega+i\Gamma)}{v_F^2q^2}\\ &\times\frac{(\omega+i\Gamma)-\left[(\omega+i\Gamma)^2-v_F^2q^2\right]^{1/2}}{\left[(\omega+i\Gamma)^2-v_F^2q^2\right]^{1/2}}\,.\end{aligned} \tag{8}$$

Here v_F is the π-electrons velocoty at the Fermi level. In the case $\omega \gg v_F q$, Eq. (8) is reduced to (3).

Let us analyze surface electromagnetic modes in two graphene layers separated by the distance l. Magnetic field of the TM wave can be written as

$$\begin{aligned}&H_y = \exp\{iqx\}\\ &\times\begin{cases} a\exp\{-ik_z z\}\,, & z<0,\\ c_1\exp\{ik_z z\}+c_2\exp\{-ik_z z\}\,, & 0<z<l,\\ d\exp\{ik_z(z-l)\}\,, & z>l.\end{cases}\end{aligned} \tag{9}$$

In regions before ($z<0$) and after ($z>l$) structure, system (9) contains only waves exponentially decaying with the distance from graphene. The boundary conditions allowing evaluation of four coefficients a, d, c_1, c_2 are given by:

$$\begin{aligned}&c_1-c_2+a=0\,,\\ &c_1+c_2-a(1+\sigma_0')=0\,,\\ &c_1\exp\{-\sqrt{q^2-\omega^2/c^2}l\}\\ &\quad -c_2\exp\{\sqrt{q^2-\omega^2/c^2}l\}-d=0\,,\\ &c_1\exp\{-\sqrt{q^2-\omega^2/c^2}l\}\\ &\quad +c_2\exp\{\sqrt{q^2-\omega^2/c^2}l\}-d(1+\sigma_0')=0\,,\end{aligned} \tag{10}$$

where, as in previous section, $\sigma_0' = (4\pi/\omega)k_z\sigma'$ and σ' is given by Eq. (8) under assumption $g_s, g_v = 2$. The resulting dispersion equation

$$2+\sigma_0'\pm\sigma_0'\exp\{-\sqrt{q^2-\omega^2/c^2}l\}=0 \tag{11}$$

manifests appearance of optical and acoustic modes (upper and lower signs, respectively). At distances l much less than the wavelength, acoustic mode slows down much

faster. This is because the terms proportional to conductivity in (11) are mutually suppressed in that case. Thus, in acoustic mode the wavenumber q must be sufficiently large in order to satisfy the dispersion equation.

Figure 5 presents the phase velocity dependence of the surface asymmetric electromagnetic mode on frequency.

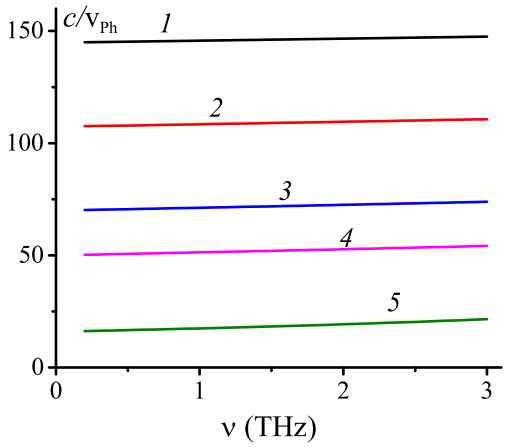

FIG. 5: Phase velocity slowing down for the acoustic mode in structure with two graphene layers. In curves $1-5$, the distances between layers are 10 nm,20 nm, 50 nm, 100 nm and 1μm, respectively. Chemical potential in all cases is $\mu = 0.1$ eV.

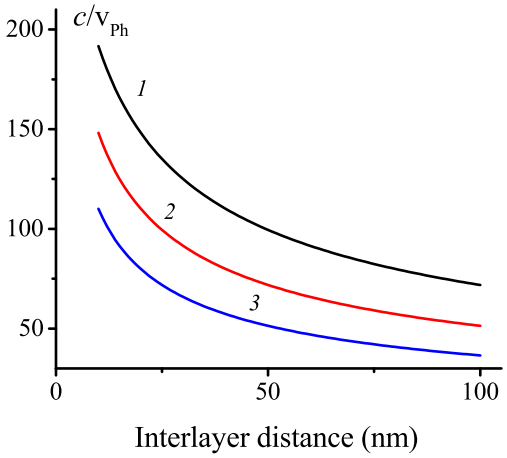

FIG. 6: The acoustic mode slowing down as a function of interlayer distance in double graphene structure at different values of chemical potential: $\mu = 0.05$(curve *1*), 0.1 (curve *2*), 0.2 (curve *3*)

Comparing the curves on this plot with curve 2 from Fig. 2 which has been plotted for the single layer at the same value of chemical potential $\mu = 0.1$ eV, one can see that the the acoustic mode slows down in double-layer structure much faster than in monolayer graphene. Figure 5 also demonstrate a weak frequency dependence of the slowing down factor in the range considered. On the contrary, the dependence of this factor on interlayer distance is essential, see Fig. 6. This gives us a tool of the effect control by varying the distance.

There is also optical mode in the double-layer structure under consideration ("+" in (11)). When wavelength exceeds significantly the interlayer distance, the dispersion equation of optical mode differs from the single-layer case in that only that chemical potential should be doubled in all expressions. In particular, this means that the slowing down of this mode is less than in a single graphene layer. When intertlayer distance is considerably less then the wavelength, it can easily be seen that for optical mode which corresponds to sign "+" in (11), the effective sheet conductivity is doubled as compared to the case of graphene monolayer. Analogous effect holds true for sandwich graphene structure with number of layers more then two. For this case, effective conductivity is equal to sum of layers conductivities. Such an additivity has been observed experimentally in studying of electromagnetic wave transmission through sandwich graphene structures[47,48].

Note that in the above consideration we restricted ourselves to the case $\mu \gg T$. When this inequality is violated, the system can be described by the effective chemical potential

$$\mu_{eff} = 2T \log\left[2\cosh\left(\frac{\mu}{2T}\right)\right], \qquad (12)$$

as it can easily be deduced from (3)and (8). Figure 7 shows temperature dependence of the ratio μ_{eff}/μ for different values of chemical potentials. One can see that temperature has low influence on the ratio for $\mu > 0.1$ eV up to PMMA melting point. what is why in our transmission/absorption experiments with CVD graphene[47,48], where chemical potential was estimated as $\mu \sim 0.14-0.17$ eV, we did not observe temperature dependence. More "pure" graphene is expected to be more sensitive to temperature change.

V. DISPERSION EQUATION IN GRAPHENE STRUCTURES IN THE PRESENCE OF ELECTRON BEAM

Let the electron beam of the width δ propagates on the distance h from the two-layer graphene structure. The dispersion equation can be derived in the manner described in the previous section. The difference consists in the appearance of additional region occupied by the electron beam. In this region the z-projection of the wavevector is given by:

$$k_{bz} = k_z\sqrt{1 - \frac{\omega_l^2}{\gamma^3(\omega - qu)^2}}, \qquad (13)$$

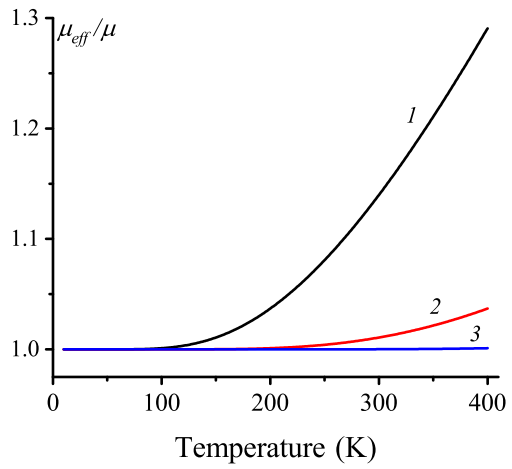

FIG. 7: Temperature dependence of the effective chemical potential for different values of chemical potential: $\mu = 0.05$(curve *1*), 0.1 (curve *2*), 0.2 (curve *3*)

where $\omega_L = \sqrt{4\pi e^2 n_e/m_e}$ is the Langmuir frequency of the electron beam and $\gamma = 1/\sqrt{1-u^2/c^2}$ its Lorentz factor, u is the velocity of electrons, n_e is the electron density and e and m_e are the electron charge and mass.System of boundary conditions in this case is discussed in Appendix A. It leads to the following dispersion equation

$$I_b = -\frac{(2+\sigma_0')^2 - (\sigma_0')^2 \exp\{-2\sqrt{q^2-\omega^2/c^2}\,l\}}{\sigma_0'\left[2+\sigma_0' + \exp\{-2\sqrt{q^2-\omega^2/c^2}\,l\}(2-\sigma_0')\right]}, \tag{14}$$

where

$$I_b = \exp(2ik_z h) \times \frac{(k_{bz}^2 - k_z^2)\left\{\exp(ik_{bz}\delta) - \exp(-ik_{bz}\delta)\right\}}{(k_{bz}-k_z)^2 \exp(ik_{bz}\delta) - (k_{bz}+k_z)^2 \exp(-ik_{bz}\delta)}.$$

It is obvious, that in the case when distance between layers significantly exceeds the distance of the surface wave dumping, the above dispersion equation is reduced to the equation for a single layer. Mathematically this is achieved by neglecting small exponential terms in numerator and denominator in the right part of (14).

As an example, we depicted in Fig. 8 the instability increment (imaginary part of the surface wave tangential wavenumber q) as a function of the frequency. Negativity of the increment is the necessary condition of the generation start. In the figure we compare the frequency dependencies for sandwich structures with 4, 8 and 9 graphene layers at $\mu = 0.2$ eV in each layer. All curves are characterized by pronounced minima at the Čerenkov resonant frequencies (generation frequencies) with the linewidths dictated by the broadening parameter. These frequencies appear to be in the THz range and significantly shift to short-wave side with the number of graphene layers. Simultaneously, the increment strongly growth in absolute value. Maximal absolute values of the instability increments presented in Figs. 8 show us that the strong amplification regime can already be realized at the interaction length of the order of several centimeters. At smaller lengthes, incorporation into the system of a feedback (for example, mirror) allows achieving generation in the weak coupling regime.

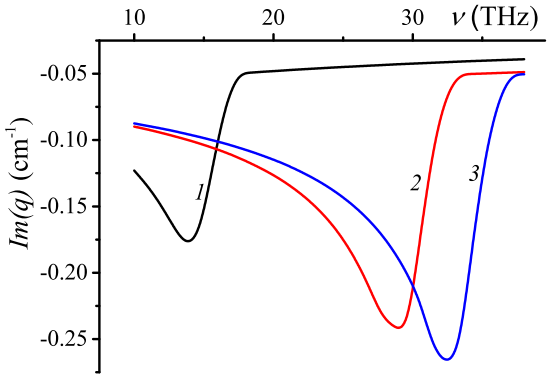

FIG. 8: Frequency dependence of the instability increment ($Im(q)$) for 4 (1), 8 (2) and 9 (3) graphene layers with chemical potential of a single layer $\mu = 0.2$ eV. Electron beam energy $E = 10$ keV, $\Gamma = 10$ THz.

Figure 9 demonstrates the increment frequency dependencies for graphene monolayer at smaller electron beam energy and two different chemical potential. In this case the generation frequency is reduced to several terahertz with simultaneous dropping the increment absolute value. Thus, multilayer graphene sandwich provides us with much better generation conditions as compared with the monolayer and admits resonant frequency tuning.

VI. CONCLUSION

In the present paper, we have studied propagation in graphene sandwich structures of surface waves exited by an electron beam moving over the sandwich surface. We have demonstrated existence in the multi-layered structure of strongly slowed down acoustic mode which allows synchronization of the beam and the surface wave at much less beam energy. Moreover, a smooth frequency tuning becomes possible by varying the system parameters, such as beam energy, chemical potential and interlayer distance.

At a given beam energy the frequency can smoothly be tuned by varying the chemical potential μ by means of electrostatic doping, see Fig. 3. At a fixed chemical potential the tuning is attained by the electron beam energy variation as is demonstrated by Fig. 4. If the graphene sandwich structure allows alteration of the in-

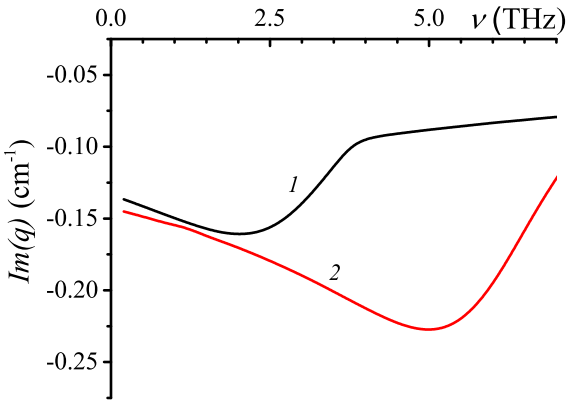

FIG. 9: Frequency dependence of the instability increment ($Im(q)$) for a single graphene layer. Electron beam energy $E = 4$ keV, chemical potential is $\mu = 0.1$ eV (1) and $\mu = 0.2$ eV (2).

terlayer distance, the spectrum tuning can be realized even at a fixed chemical potential and beam energy, see Fig. 5. This is because in multi-layered graphene structures there are electromagnetic modes whose phase velocities can be both essentially smaller and exceed the the surface wave phase velocity reachable in a single-layer graphene. All the factor mentioned allow matching the electron beam energy, the chemical potential and the interlayer distance (and number of layers) to synchronize electron beam and surface electromagnetic wave at a fixed frequency, while external electrostatic field (electrostatic doping) provides additional possibility for fine frequency tuning.

It should be emphasized that the graphene layers in sandwich should not be obligatory whole. In order to provide interaction of the electron beam with the graphene on the several centimeters length, it is sufficient to have a mosaic surface comprising disoriented in plane graphene blocks. Moreover, since cylindrical and tubular beams are widespread in electronic engineering, planar geometry considered in the present paper (see Fig. 1) can easily be rearranged to cylindrical by, for example, stacking graphene layer on a cylinder.

Thus, based on the analysis carried out, one can conclude that multi-layered graphene/dielectric structures with negligible interlayer tunnelling provide enhanced conditions for the terahertz Čerenkov radiation generation excited by an external non-relativistic electron beam. New methods of the generation frequency tuning can be realized by varying the graphene doping, the number of graphene sheets, the distance between sheets, etc.

Acknowledgments

This publication is based on work supported by a grant from the U.S. Air Force under Agreement FA9550-15-D-0003. Authors also acknowledge a support from EU FP7 project FP7-612285 CANTOR and EU Horizon 2020 project H2020-644076 CoExAN.

Appendix A: Electron beam accounting

Consider electron beam propagating over some plane structure, see Fig. 1. In further consideration we make use the procedure developed in Ref. 54. Linealized equations describing electron beam dynamics are well-known and given by:

$$\begin{array}{l} \dfrac{\partial \delta v_x}{\partial t} + u\dfrac{\partial \delta v_x}{\partial x} = \dfrac{e}{m\gamma^3}E_x \\ \dfrac{\partial \delta n}{\partial t} + \dfrac{\partial}{\partial x}\left(n_0 \delta v_x + u\delta n\right) = 0 \end{array} \tag{A1}$$

Fourier transform of (A1) leads to

$$\begin{array}{l} \left(k_{bz}^2 c^2 - \omega^2\right) E_x - q k_{bz} c^2 E_z = -\dfrac{\omega_L^2 \omega^2}{\Delta^2 \gamma^3} E_x \\ -q k_{bz} c^2 E_x + \left(q^2 c^2 - \omega^2\right) E_z = 0 \end{array} \tag{A2}$$

that gives the dispersion equation as follows

$$k_b^2 c^2 - \omega^2 = \frac{\omega_L^2}{\Delta^2 \gamma^3}\left(q^2 c^2 - \omega^2\right), \tag{A3}$$

where $k_b^2 = q^2 + k_{bz}^2$ and $\Delta = \omega - qu$. Solutions of this equation is given by (13). Boundary conditions fot the electromagnetic wave (1) interacting with electron beam are produced by analogy with the case considered in Sects. III-IV by imposing conditions on tangential components of electric and magnetic fields on the boundaries. The only difference is that in the beam, the following relation dictated by Maxwell equation

$$E_x = \frac{k_{0z}^2 c}{\omega k_{bz}} H_y. \tag{A4}$$

is used for tangential components of electric and magnetic fields. Particulary, for the electron beam with the thickness δ propagating over two layer graphene on the distance h we have a system for eight coefficients. Two of them, a_1 and a_2 correspond to regions below structure and above the beam, respectively, while coefficients $c_{1,2}$ and $d_{1,2}$ describe waves inside two-layer structure and between structure and beam. Finally, coefficients $f_{1,2}$ correspond to two counter-propagating waves in the beam:

$$\begin{array}{l} H_y = \exp\{iqx\} \\ \times \begin{cases} a_1 \exp\{-ik_z z\}, & z < 0, \\ c_1 \exp\{ik_z z\} + c_2 \exp\{-ik_z z\}, & 0 < z < l, \\ d_1 \exp\{ik_z (z-l)\} & \\ \quad + d_2 \exp\{-ik_z (z-l)\}, & l < z < h, \\ f_1 \exp\{ik_{bz} z\} + f_2 \exp\{-ik_{bz} z\}, & h < z < h + \delta \\ a_2 \exp\{ik_z z\}, & z > h + \delta. \end{cases} \end{array}$$

Assuming determinant of this linear system to be zero we come to Eq. (14).

---

* Electronic address: kgbatrakov@gmail.com.

[1] R. A. Lewis, J. Phys. D **47**, 374001 (2014), DOI:10.1088/0022-3727/47/37/374001.

[2] A. Pawara, D. Sonawanea, K. Erandea, and D. Derleb, Drug Invention Today **5**, 157 (2013), DOI:10.1016/j.dit.2013.03.009.

[3] A. Gilmour, *Klystrons, Traveling Wave Tubes, Magnetrons, Cross-Field Amplifiers, and Gyrotrons* (Artech House Microwave Library, 2011).

[4] T. Marshall, *Free-Electron Lasers* (Macmillan, New York, 1985).

[5] J. Walsh, Final Report DAAG29-85-K-0176, U.S. Army Research Office, Dartmouth College, Hanover N.H. (1988).

[6] K. Novoselov, A. Geim, S. Morozov, D. Jiang, Y. Zhang, S. Dubonos, I. Grigorieva, and A. Firsov, Science **306**, 666 (2004), DOI: 10.1126/science.1102896.

[7] A. M. Nemilentsau, M. V. Shuba, G. Y. Slepyan, P. P. Kuzhir, S. A. Maksimenko, P. N. D'yachkov, and A. Lakhtakia, Phys. Rev. B **82**, 235424 (2010), URL http://link.aps.org/doi/10.1103/PhysRevB.82.235424.

[8] M. A. Kanygin, O. V. Sedelnikova, I. P. Asanov, L. G. Bulusheva, A. V. Okotrub, P. P. Kuzhir, A. O. Plyushch, S. A. Maksimenko, K. N. Lapko, A. A. Sokol, et al., Journal of Applied Physics **113**, 144315 (2013), URL http://scitation.aip.org/content/aip/journal/jap/113/14/10.1063/1.4800897.

[9] G. Y. Slepyan, S. A. Maksimenko, A. Lakhtakia, O. Yevtushenko, and A. V. Gusakov, Phys. Rev. B **60**, 17136 (1999), DOI: 10.1103/PhysRevB.60.17136.

[10] K. Batrakov, V. Saroka, S. Maksimenko, and C. Thomsen, J. Nanophotonics **6**, 061719 (2012), DOI: 10.1117/1.JNP.6.061719.

[11] K. Batrakov, P. Kuzhir, and S. Maksimenko, in *Proceedings of SPIE - The International Society for Optical Engineering*, edited by A. Lakhtakia and S. Maksimenko (SPIE Digital Library, San Diego, California, USA, 2006), vol. 6328, p. 63280Z, DOI: 10.1117/12.678029.

[12] K. Batrakov, P. Kuzhir, and S. Maksimenko, Physica E **40**, 2370 (2008), DOI: 10.1016/j.physe.2007.07.029.

[13] K. Batrakov, P. Kuzhir, and S. Maksimenko, Physica E **40**, 1065 (2008), DOI: 10.1016/j.physe.2007.08.003.

[14] K. Batrakov, P. Kuzhir, S. Maksimenko, and C. Thomsen, Phys. Rev. B **79**, 125408 (2009), DOI: 10.1103/PhysRevB.79.125408.

[15] K. Batrakov, O. Kibis, P. Kuzhir, C. Rosenau, and M. Portnoi, J. Nanophotonics **4**, 041665 (2010), DOI: 10.1117/1.3436585.

[16] M. Jablan, M. Soljacic, and H. Buljan, Proceedings of the IEEE **101**, 1689 (2013), DOI: 10.1109/JPROC.2013.2260115.

[17] V. Ryzhii, V. Ryzhii, and T. Otsuji, J. Appl. Phys. **101**, 083114 (2007), DOI: 10.1063/1.2717566.

[18] V. Ryzhii, A. Dubinov, T. Otsuji, V. Mitin, and S. M.S, J. Appl. Phys. **107**, 054505 (2010), DOI: 10.1063/1.3327212.

[19] A. Dubinov, V. Aleshkin, V. Mitin, T. Otsuji, and V. Ryzhii, J. Physics: Condensed Matter **23**, 145302 (2011), DOI:10.1088/0953-8984/23/14/145302.

[20] V. Ryzhii and V. Ryzhii, Japan. J. Appl. Phys. **46**, L151 (2007).

[21] F. Rana, IEEE Trans. Nanotechnol. **7**, 91 (2008), DOI: 10.1109/TNANO.2007.910334.

[22] F. J. G. de Abajo, ACS Nano **7**, 11409 (2013), DOI: 10.1021/nn405367e.

[23] I. Kaminer, Y. T. Katan, H. Buljan, Y. Shen, O. Ilic, J. Lopez, L. Wong, J. Joannopoulos, and M. Soljacic, NATURE COMMUNICATIONS **7**, 1 (2016), DOI: 10.1038/ncomms11880.

[24] O. V. Kibis and M. E. Portnoi, Techn. Phys. Lett. **31**, 671 (2005), ISSN 1090-6533, URL http://dx.doi.org/10.1134/1.2035361.

[25] O. V. Kibis, D. G. W. Parfitt, and M. E. Portnoi, Phys. Rev. B **71**, 035411 (2005), URL http://link.aps.org/doi/10.1103/PhysRevB.71.035411.

[26] O. V. Kibis, M. R. da Costa, and M. E. Portnoi*, Nano Letters **7**, 3414 (2007), pMID: 17967042, http://dx.doi.org/10.1021/nl0718418, URL http://dx.doi.org/10.1021/nl0718418.

[27] K. Batrakov, O. Kibis, P. Kuzhir, S. Maksimenko, D. C. M. Rosenau, and M. Portnoi, Physica B **405**, 3054 (2010), DOI: 10.1016/j.physb.2010.01.048.

[28] R. R. Hartmann, J. Kono, and M. E. Portnoi, Nanotechnology **25**, 322001 (2014), URL http://stacks.iop.org/0957-4484/25/i=32/a=322001.

[29] S. Mikhailov, Phys. Rev. B **87**, 115405 (2013), DOI: 10.1103/PhysRevB.87.115405.

[30] A. Moskalenko and S. Mikhailov, J. Appl. Phys. **115**, 203110 (2014), DOI: 10.1063/1.4879901.

[31] T. Zhan, D. Han, X. Hu, X. Liu, S.-T. Chui, and J. Zi, Phys. Rev. B **89**, 245434 (2014), URL http://link.aps.org/doi/10.1103/PhysRevB.89.245434.

[32] S. Liu, C. Zhang, M. Hu, X. Chen, P. Zhang, S. Gong, T. Zhao, and R. Zhong, Applied Physics Letters **104**, 201104 (2014), URL http://scitation.aip.org/content/aip/journal/apl/104/20/10.1063/1.4879017.

[33] N. R. Sadykov, E. A. Akhlyustina, and D. A. Peshkov, Theoretical and Mathematical Physics **184**, 1163 (2015), DOI: 10.4213/tmf8831.

[34] N. R. Sadykov, A. V. Aporoski, and D. A. Peshkov, Optical and Quantum Electronics **48**, 358 (2016), DOI: 10.1007/s11082-016-0625-8.

[35] Z. Yao, C. L. Kane, and C. Dekker, Phys. Rev. Lett. **84**, 2941 (2000), URL http://link.aps.org/doi/10.1103/PhysRevLett.84.2941.

[36] B. Q. Wei, R. Vajtai, and P. M. Ajayan, Applied Physics Letters **79**, 1172 (2001), URL http://scitation.aip.org/content/aip/journal/apl/79/8/10.1063/1.1396632.

[37] R. Murali, Y. Yang, K. Brenner, T. Beck, and J. D. Meindl, Applied Physics Letters **94**, 243114 (2009), URL http://scitation.aip.org/content/aip/journal/apl/94/24/10.1063/1.3147183.

[38] C. Berger, Y. Yi, Z. L. Wang, and W. A. de Heer, Appl. Phys. A **74**, 363 (2002), DOI: 10.1007/s003390201279.

[39] P. Poncharal, C. Berger, Y. Yi, Z. L. Wang, and W. A. de Heer, J. Phys. Chem. B **106**, 12104 (2002), DOI: 10.1021/jp021271u.

[40] C. Berger, P. Poncharal, Y. Yi, and W. A. de Heer, J. Nanosci. Nanotechnol. **3**, 171 (2003).

[41] Y. Yi, PhD dissertation, Georgia Institute of Technology, Georgia, USA (2004), Ballistic Conduction in Multiwalled Carbon Nanotubes at Room Temperature.

[42] J. Baringhaus, M. Ruan, F. Edler, A. Tejeda, M. Sicot, A. Taleb-Ibrahimi, A.-P. Li, Z. Jiang, E. H. Conrad, C. Berger, et al., Nature **506**, 349 (2014), DOI: 10.1038/nature12952.

[43] O. Klein, J. Nanosci. Nanotechnol. **53**, 157165 (1929), DOI: 10.1007/BF01339716.

[44] M. I. Katsnelson, K. S. Novoselov, and A. K. Geim, Nature Physics **2**, 620 (2006), DOI: 10.1038/nphys384.

[45] I.-T. Lin and J.-M. Liu, Applied Physics Letters **103**, 201104 (2013), DOI: 10.1063/1.4830006.

[46] P. Alonso-Gonzalez, A. Y. Nikitin, Y. Gao, A. Woessner, M. B. Lundeberg, A. Principi, N. Forcellin, W. Yan, S. Velez, A. J. Huber, et al., Nature Nanotechnology pp. 31–36 (2016), DOI: 10.1038/nnano.2016.185.

[47] K. Batrakov, P. Kuzhir, S. Maksimenko, A. Paddubskaya, S. Voronovich, P. Lambin, T. Kaplas, and Y. Svirko, Scientific Reports **4**, 7191 (2014), DOI: 10.1038/srep07191.

[48] K. Batrakov, P. Kuzhir, S. Maksimenko, A. Paddubskaya, S. Voronovich, G. Valusis, T. Kaplas, Y. Svirko, and P. Lambin, Appl. Phys. Lett. **108**, 123101 (2016), DOI: 10.1063/1.4944531.

[49] S. A. Mikhailov, in *Carbon nanotubes and graphene for photonic applications*, edited by S. Yamashita, Y. Saito, and J. H. Choi (Woodhead Publishing, Cambridge CB22 3HJ, UK, 2013), chap. 7, pp. 171–219.

[50] A. H. C. Neto, F. Guinea, N. M. R. Peres, K. S. Novoselov, and A. K. Geim, Rev. Modern Phys. **81**, 109 (2009), DOI: 10.1103/RevModPhys.81.109.

[51] S. D. Sarma and E. H. Hwang, Phys. Rev. Lett. **102**, 206412 (2009), DOI: 10.1103/PhysRevLett.102.206412.

[52] E. M. Lifshitz and L. P. Pitaevskii, *Physical Kinetics*, vol. 10 of *Course of Theoretical Physics* (Pergamon Press, Oxford, 1981), 1st ed.

[53] S. A. Mikhailov and K. Ziegler, Phys. Rev. Lett. **99**, 016803 (2007), DOI: 10.1103/PhysRevLett.99.016803.

[54] L. Schächter and A. Ron, Phys. Rev. A **40**, 876 (1989), URL `http://link.aps.org/doi/10.1103/PhysRevA.40.876`.